Supplement

S.1 Roll milling process

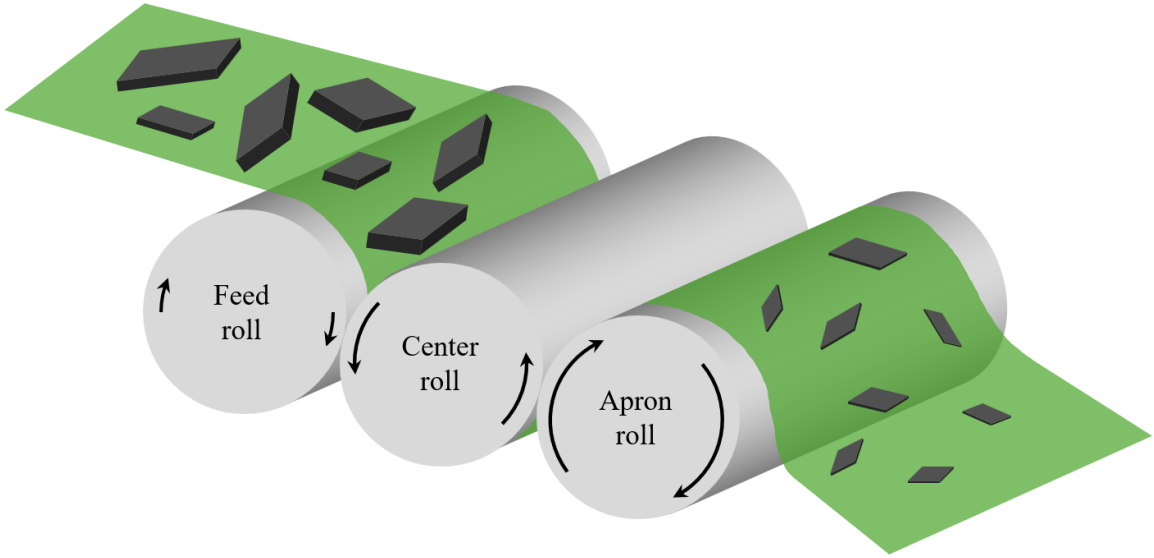

Figure S1 Schematic diagram of the three-roll mill.

S.2 Thermal conductivity measuring device

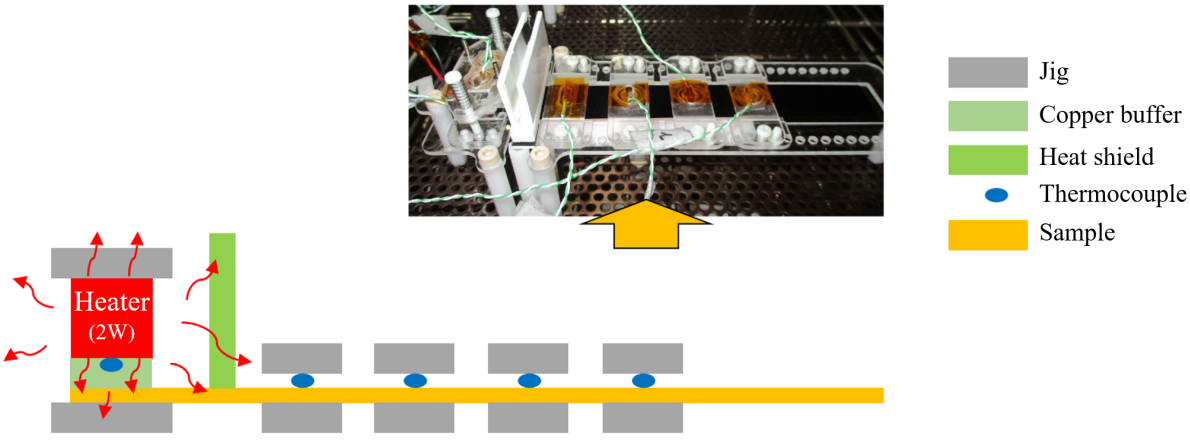

Figure S2 Appearance and schematic diagram of the thermal conductivity measuring device.

S.3 Viscosity measurement

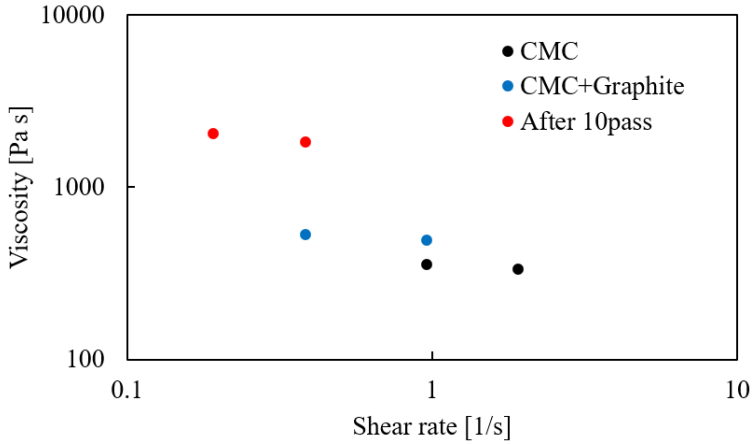

Figure S3 Viscosity of the solution at each step.

S.4 Particle size measurement details

To measure the particle size of the produced graphite, a mixture with an extremely dilute graphite concentration of pure water : CMC : graphite = 20 : 0.1415 : 0.0085 was made after processing with a roll mill, and after film formation and drying by blade coating at a blade height of 0.4 mm, images are taken with an optical microscope at x20, x200 and x2000 respectively, as shown in Fig.S4. Particles with a size between 1.67 and 15 μm are measured from images at 2000x, particles with a size between 15 and 135 μm from images at 200x and particles with a size greater than 135 μm from images at 20x, and the size and number of particles is determined by image processing software. The average number of particles taken from a single image measured at each magnification is then adjusted to the unit area (e.g. if the unit area is the range of images at 20x in Fig.S4, the number of particles measured at 200x is multiplied by 100 and the number of particles measured at 2000x is multiplied by 10 000). Finally, as averaging by number gives a histogram that is far removed from the actual effect of each particle, as shown in Fig.S4(d), the particle aspect ratio of all particles was set to a similarity of 1000 and the volume fraction of each particle size range was calculated and made into a histogram. Due to the convenience of measuring with an optical microscope, it was not possible to measure particles with a diameter of 1.67 or less, but the trend in the histogram in Fig.3(a) shows that the volume fraction of particles with a particle size of 1.67 or less is expected to be very low. In fact, a comparison of Fig.2(c) and Fig.3(a) shows that this method of evaluation makes more sense than taking the average by number of particles.

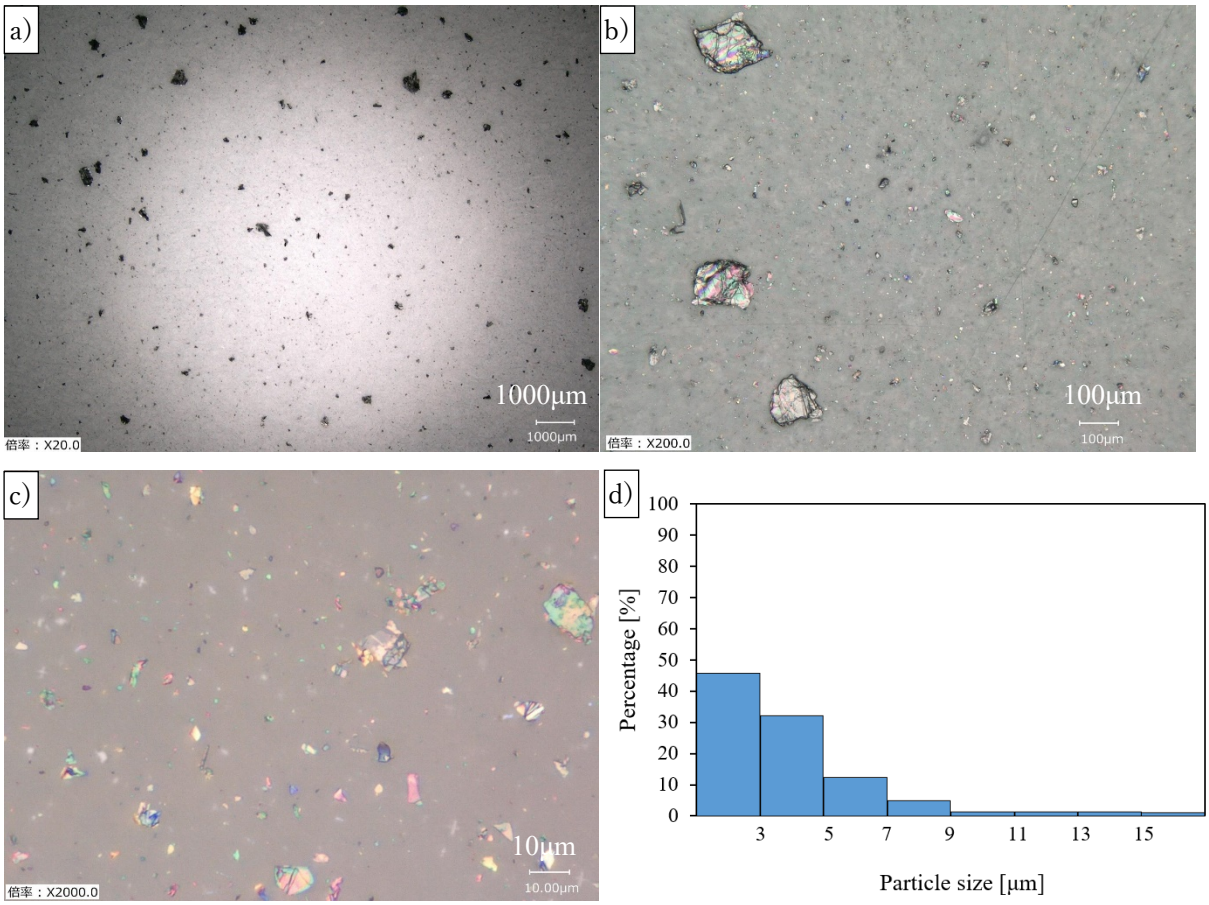

Figure S4 Particle size measurement details. a)-c) Optical microscope image of film for particle size measurement, a) ×20, b) ×200, c) ×2000, d) Histogram of particle size of 10 passes

S.5 Particle size distribution measured by TEM and exfoliation measured by absorbance

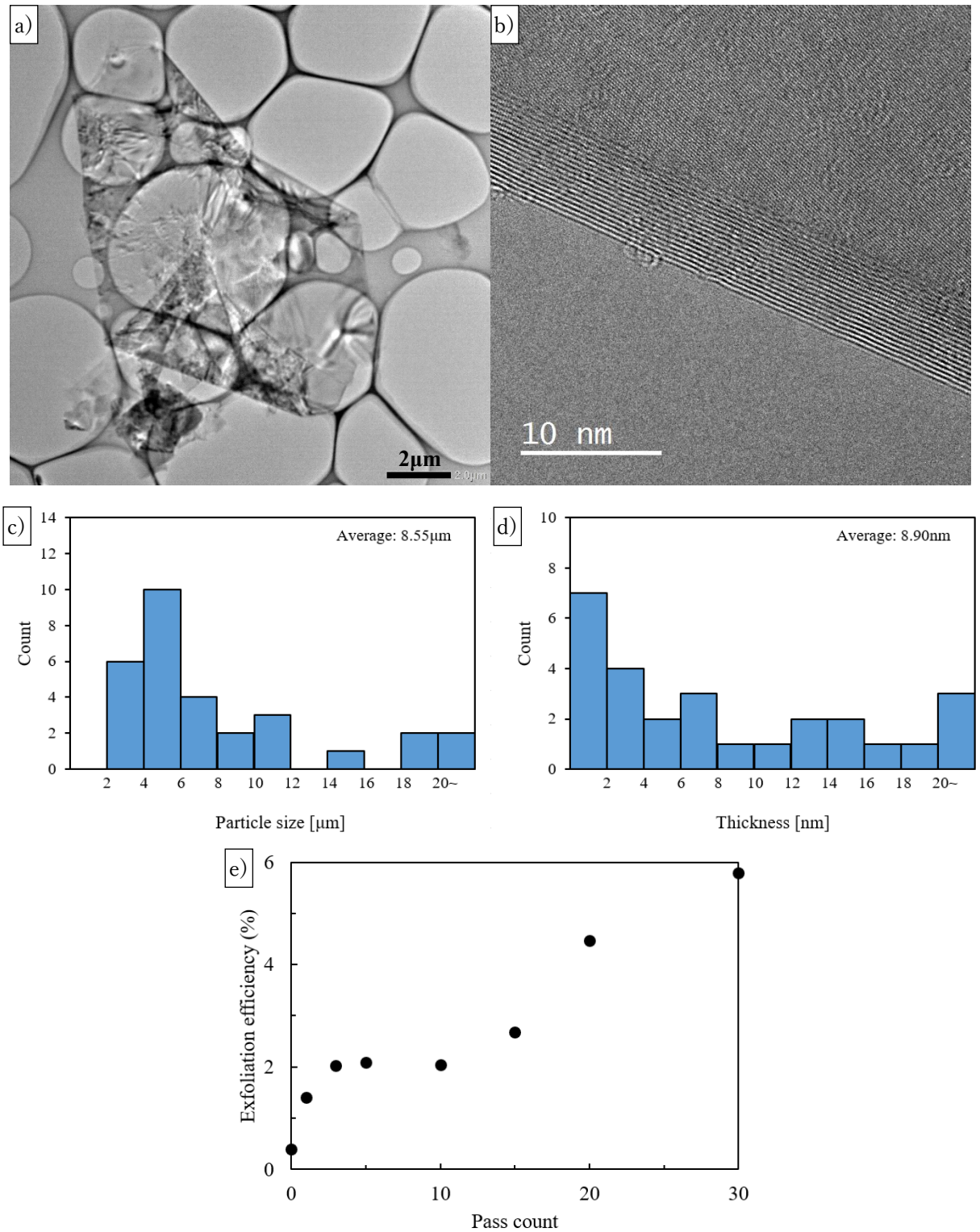

Figure S5 Particle size distribution measured by TEM and exfoliation measured by absorbance. a)-d): graphite content 85%, 10pass. a) TEM image for particle size measurement, b) TEM image for thickness measurement, c) Histogram of particle size measured by TEM, d) Histogram of thickness measured by TEM, e) Exfoliation efficiency by number of passes.

S.6 Evaluation of graphite crystallinity by Raman

The crystallinity of graphite was measured using a Raman microscope (inVia RefleX, RENISHAW Co.,Ltd.). Fig.S6 a) is an image of the film surface taken with the optical microscope accompanying the Raman microscope and b) is an I_D/I_G mapping of the same area. The black areas in a) are CMC in which GNP are dispersed and the white areas are graphite flakes. The white areas in a) are in good agreement with the black areas in b) (I_D/I_G close to 0.01), indicating that the graphite flakes are well crystallized and almost free of defects. The Raman spectra of 20 graphite flakes were measured and the average of I_D/I_G was determined to be 0.026.

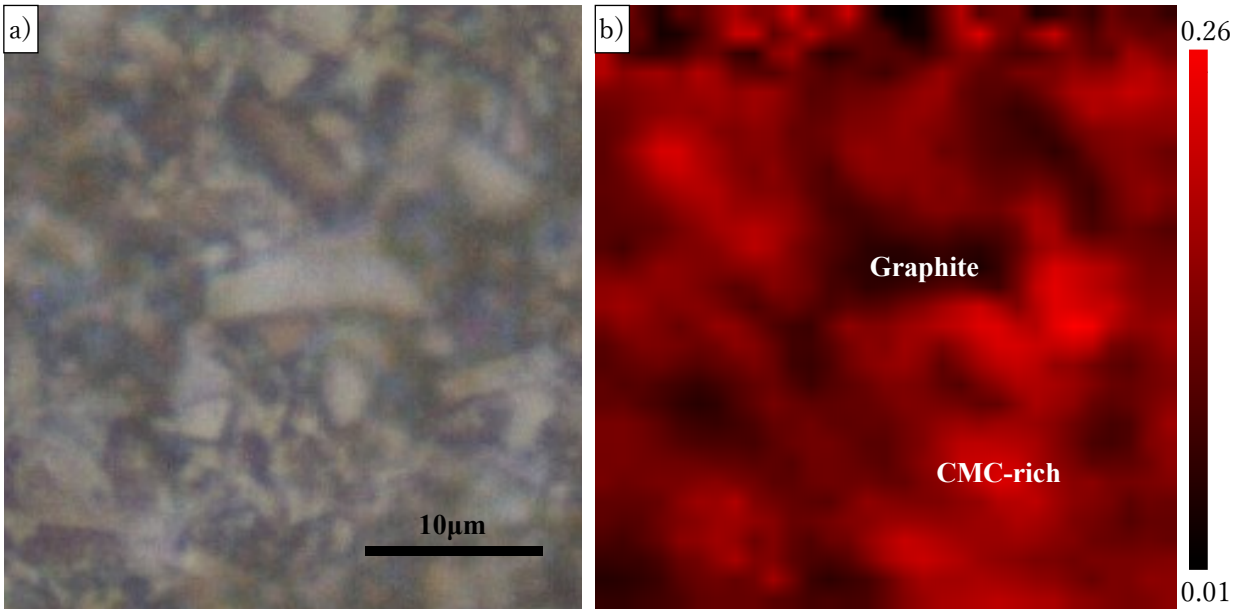

Figure S6 Evaluation of graphite film surface crystallinity. a) Optical microscope image of film surface, b) I_D/I_G mapping in the same range.

S.7 Thickness measurement details

The thickness of the graphite produced was measured by observing the cross-section of the film by FE-SEM. A single image was taken where the entire thickness direction of the sample was visible, as in Fig.S7(a). A single vertical line was drawn at a random point, and all graphite flakes through which the line passed, from the bottom to the top, were enlarged to a magnification where the thickness of the particles could be seen, as in Fig.S7(b)(c), and the thickness was measured. If a crack appeared in the graphite flake in the enlarged image and it was difficult to determine whether it was a single particle or not, it was judged by comparing it with the first image taken where the entire thickness direction of the sample was visible. To see the actual effect of each thickness range, thickness percentages were calculated in the histogram and are shown in Fig.S7(e). In addition, thicknesses of less than 20 nm were not included in the measurements in this study. As in section **Error! Reference source not found.**, this is not only difficult to measure in terms of resolution, but also there are hardly any particles with a thickness of 20 nm or less to look for (it is not because they are thin that they are invisible).Fig.S7(c) shows the area where the average thickness is thin and Fig.S7(d) is an enlargement of a part of it (red square area). Looking at the red circles in Fig.S7(d), it is possible to observe those that are even too thin to measure the thickness, if they exist. However, as far as the samples are concerned, there are almost no such particles, and comparing Fig.2(c) and Fig.S7(e), it can be seen that this evaluation method, which takes the thickness percentage of objects with a thickness of 20 nm or more is reasonable.

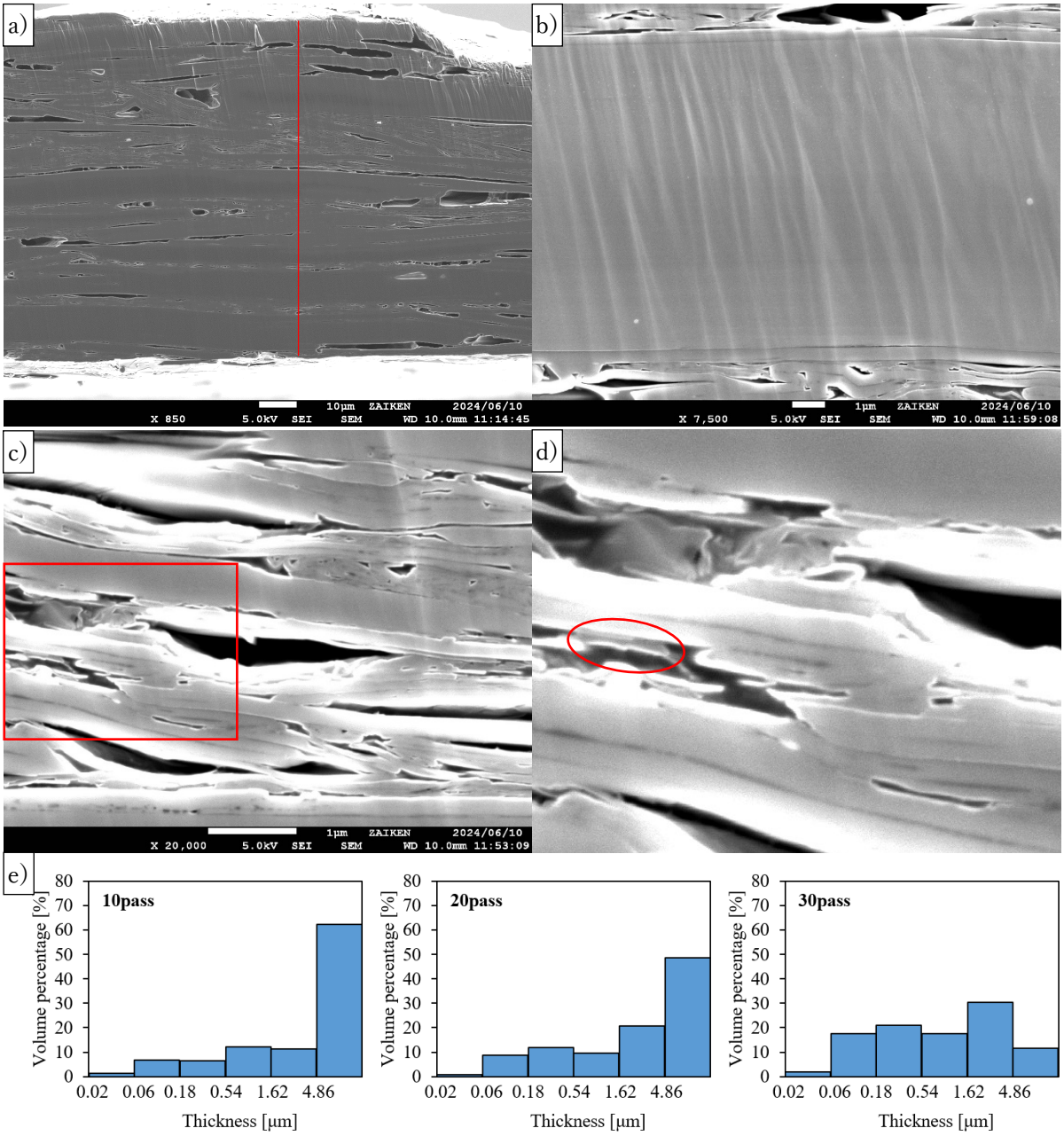

Figure S7 Methods and results of thickness measurement of graphite flakes. a)-d) SEM image of cross-section for thickness measurement, e) Histogram of thickness.

S.8 Graphene film data

Fig.S8 shows the results of the calculation of the change in thermal conductivity when each parameter was replaced by that the graphite film. For example, for the line whose name is aspect ratio, only the aspect ratio is calculated with reference to the value of graphite in Table S1, while the other values are calculated with reference to the GNP.

Table S1 Setting of material constants

Material constant	Unit	Graphite	GNP
Thermal conductivity of the composite in the in-plane direction	$Wm^{-1}K^{-1}$	1200	1200
Thermal conductivity of the composite in the out-of-plane direction	$Wm^{-1}K^{-1}$	12	12
Statistical orientation $<\cos^2\theta>$	/	0.97	0.90
Aspect ratio	/	1000	3500
Density of the film	/	theoretical density×0.9	theoretical density×0.8
Interfacial thermal resistance R_k	m^2KW^{-1}	5.0×10^{-8}	7.5×10^{-8}
Particle size of filler B	μm	Table S2	25

Table S2 Particle size of exfoliated graphite (85%, 10pass)

Particle size μm	Volume percentage %
3.05	0.535
7.65	2.27
26.2	5.22
78.2	15.0
206	39.6
471	37.4

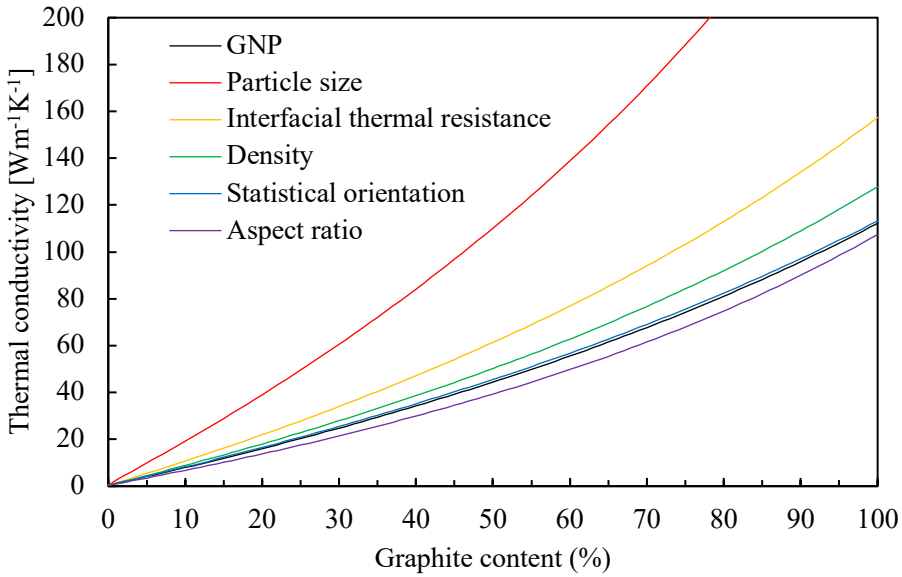

Figure S8 Change in theoretical value when only one material constant is changed.

Table S3 Particle size distribution used in Fig.S9.

Type 1		Type 2		Type 3	
Particle size μm	Volume percentage %	Particle size μm	Volume percentage %	Particle size μm	Volume percentage %
3.05	0.535	6.70	16.7		
7.65	2.27	13.4	16.7		
26.2	5.22	40.2	16.7		
78.2	15.0	121	16.7	271	100
206	39.6	362	16.7		
471	37.4	1085	16.7		

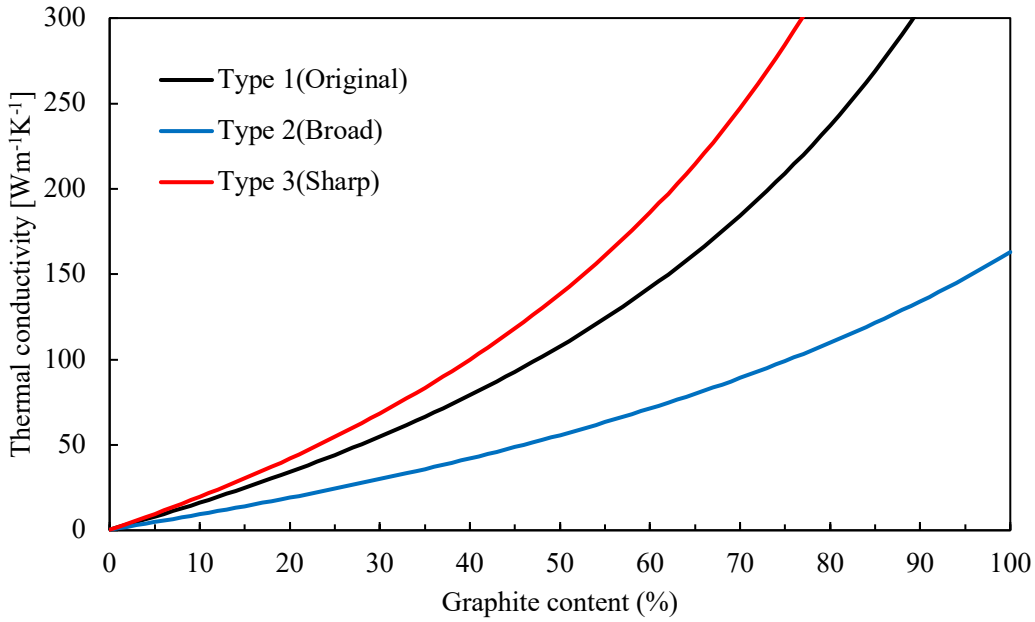

Figure S9 The effect of varying particle size distribution on thermal conductivity.

S.9 Thermography

Thermography was measured using the equipment in Fig.S10. The width of sample was 10mm, and the distance between the heat sink and heat source was 50mm.

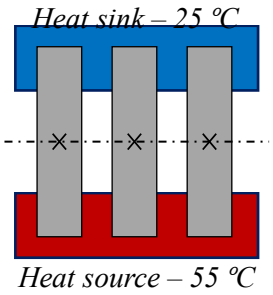

Figure S10 Schematic diagram of the thermography measurements

S.10 Micro voids and particle folding/wrinkling in GNP film

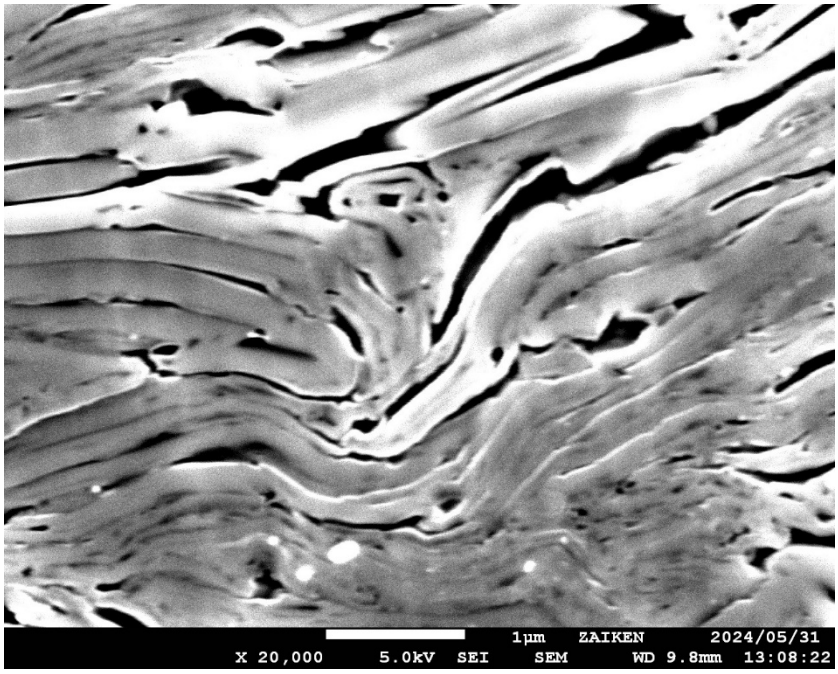

Figure S11 Micro voids and particle folding/wrinkling in GNP films after press

S.11 Measurement of orientation

To quantitatively measure the orientation of graphite in the produced films, measurements were made using a Automated Multipurpose X-ray Diffractometer With Guidance Software (SmartLab 9kW, RIGAKU Co.,Ltd). Specifically, the 2θ/θ measurement (out-of-plane measurement) was first made to measure the 2θ of the (002) plane of graphite, which was then fixed and the χ measurement was made at 0-75 degrees. An example of the measurement data is shown in Fig.S12, and this data is used to calculate the statistical orientation <cos2θ> in Equation (S1). Due to the construction of the equipment, it is not possible to measure after 75 degrees, but the measurement data shows that the intensity after 75 degrees is almost zero, so the intensity after 75 degrees is calculated as zero when calculating with Equation (S1). The measurement results for each sample are shown in Table S4.

$$< \cos^2 \theta >= \frac{\int_0^{90} I \cos^2 \theta \sin \theta \, d\theta}{\int_0^{90} I \sin \theta \, d\theta} \quad \text{(S1)}$$

where I is the intensity after normalization and θ is the angle of rotation of the sample along the χ axis.

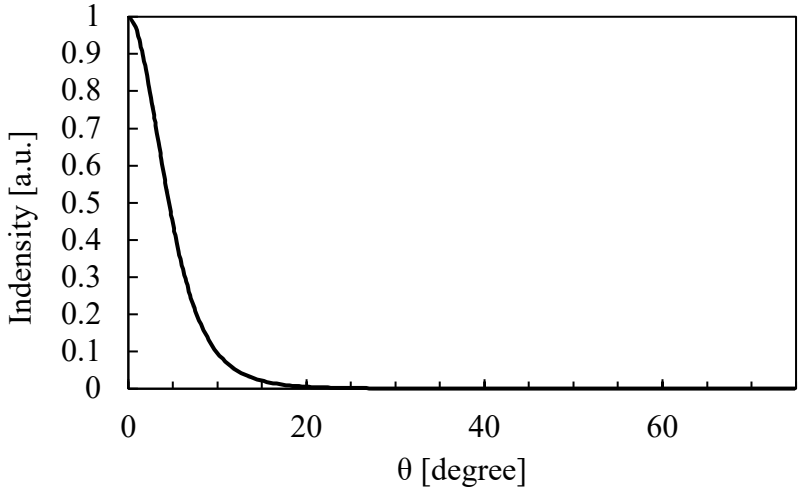

Figure S12 χ measurement results for graphite film. (85%, 10pass)

Table S4 Statistical orientation of each film

	$\langle\cos^2\theta\rangle$
Gr55	0.9656
Gr70	0.9723
Gr85	0.9724
GNP55	0.9117
GNP70	0.8896
GNP85	0.9043